Atomic structure and bonding in liquid GaAs from *ab initio* molecular dynamics

Q.-M. Zhang, G. Chiarotti, and A. Selloni
International School for Advanced Studies, strada Costiera 11, I-34100 Trieste, Italy

R. Car
International School for Advanced Studies, strada Costiera 11, I-34100 Trieste, Italy
and Laboratorio di Tecnologie Avanzate di Superfici e Catalisi (TASC)
del Consorzio Interuniversitario per la Fisica della Materia (INFM), Area di Ricerca, Padriciano 99, I-34012 Trieste, Italy

M. Parrinello
International School for Advanced Studies, strada Costiera 11, I-34100 Trieste, Italy
and IBM Research Division, Zurich Research Laboratory, CH-8803 Rüschlikon, Switzerland
(Received 6 December 1989; revised manuscript received 7 May 1990)

The structural and electronic properties of liquid GaAs are investigated using *ab initio* molecular-dynamics methods. In agreement with experiments, we find that liquid GaAs is metallic, with an average coordination number between 5 and 6. Analysis of the electronic-charge distribution shows that weakly ionic bonds, similar to those of crystalline GaAs, are still present in the liquid. At variance with the crystal, these bonds are not permanent, but are continuously formed and disrupted by atomic diffusion. On the average, however, almost 50% of the atoms of the first coordination shell are bonded to the central atom. Bonds between like atoms are very frequent ($\sim$ 27%); three-atom clusters of a single species have a relative probability of 6%, while larger clusters occur only occasionally.

I. INTRODUCTION

Recently a great deal of attention has been paid to the study of disordered semiconductors. Although most of the work is focused on the solid amorphous (a) phase, the liquid (l) phase is also attracting increasing interest, both for its basic relevance and because of the role of the liquid phase in technologically important processes such as crystal growth from the melt. While much is known theoretically and experimentally on the liquid phase of the group-IV elemental semiconductors, particularly Si and Ge, the corresponding study of the III-V compound semiconductors such as GaAs is still in its infancy. Here new phenomena are expected to come into play since, together with the positional disorder also present in the elemental semiconductors, one must consider the compositional disorder, which can give rise to chemical defects such as wrong bonds (i.e., bonds between like atoms), which are absent in the perfect crystalline phase of compound materials. Such defects are expected to have a considerable influence on optical and electronic properties. Unfortunately neutron-diffraction results have been unable to separate the three partial structure factors S_{AsAs}, S_{GaGa}, and S_{AsGa}, and have only given a linear combination of the three, weighted by the scattering lengths.[1] Since the neutron-scattering lengths of As and Ga are fairly similar,[2] the experimentally determined structure factor gives with good approximation the structure of the fluid, averaged over the two atomic species. Thus the crucial information on the relative arrangement of the atoms, and therefore on the presence of wrong bonds, is not available as yet.

Experiments show that, similar to Si and Ge, GaAs becomes metallic and increases its density upon melting.[3] Neutron-scattering data for the species-averaged structure indicate that the larger density of the liquid phase is related to a variation of the coordination number z, from the value 4 typical of the crystal to a value of approximately 5.5 ($\pm$0.5), while a slight increase of the average interatomic separation takes place.[1] This value of z is much smaller than that of simple liquid metals, where close packing gives rise to typical values of z in the range 12–14,[4] and even lower than that observed in l-Si and l-Ge, where z is between 6 and 7. This suggests that covalent (or mixed ionic and covalent) bonds in l-GaAs are likely to play an important role. A question of great interest is to understand how these bonds may coexist with the observed metallic behavior. A more specific and closely related issue concerns the origin of the small, yet observable, differences between the average structural properties of l-GaAs and those of molten Si and Ge.

We report here the results of a first-principles molecular-dynamics (MD) (Ref. 5) simulation of l-GaAs.

This method has been successfully used to investigate the liquid[6,7] and amorphous phases[8,9] of several elemental materials. A distinctive feature of the *ab initio* MD scheme is that one generates at the same time the atomic trajectories and the corresponding ground-state electronic-charge distributions. One can therefore follow directly the evolution of the chemical bonds resulting from the atomic motion. In addition, one can calculate consistently electronic properties, such as densities of states, conductivities, etc.

The results of the present calculations are in good agreement with the available experimental information. Furthermore they provide reliable information on aspects of *l*-GaAs that are not experimentally accessible, such as the separate structure factors. A rather detailed picture of the atomic and electronic structure of the liquid emerges. In particular we find that the low coordination number, $z \sim 5.5$, is to be related to the persistence of predominantly covalent bonds, as characterized by the presence of charge pileup in between pairs of atoms. At variance with the crystal, these bonds change in time due to the atomic diffusion. On the average, however, almost 50% of the atoms of the first coordination shell are bonded to the central atom, and correspondingly the average number of bonds per atom is somewhat smaller than 3 (to be compared to the value of 4 for the crystal). Of these, almost 30% are between like atoms.

By comparing the results of this work to those of a recent MD study based on pseudopotential-derived two-body interatomic forces,[10] we find a good agreement for a number of species-averaged quantities, such as the total pair correlation function, the total bond-angle distribution, and the electronic density of states. Important differences occur, instead, for quantities which depend on the spatial distribution of the two atomic species, such as the partial correlation functions. At variance with our results, the atomic arrangement is found to be chemically random in Ref. 10. This is likely related to a difficulty of the pseudopotential perturbation approach used in Ref. 10 at correctly describing the subtle chemical interactions between the different species.

We have compared our results also with those of a recent *ab initio* MD simulation for *l*-Si.[7] Several differences between *l*-GaAs and *l*-Si emerge, which are described in some detail in the following. All these differences indicate that the scattering in *l*-GaAs is stronger than in *l*-Si.

This paper is organized as follows. In Sec. II we give a short discussion of the *ab initio* method and present the equations of motion used in this work. Since detailed accounts of this method have already been given[5,11,12] we shall restrict our discussion here to a few points only. Section III discusses more technical points, concerning in particular the nonlocal pseudopotentials for Ga and As,[13,14] and their treatment within the scheme of Kleinman and Bylander.[15] In Sec. IV we present our results for the structural and electronic properties of liquid GaAs. A short summary and our conclusions are given in Sec. V.

II. EQUATIONS OF MOTION

The essential feature of the *ab initio* MD scheme is that, for each ionic configuration $\{\mathbf{R}_I\}$, the many-body potential $\Phi[\{\mathbf{R}_I\}]$—which defines the Born-Oppenheimer (BO) potential-energy surface for the ions—is obtained directly from the electronic ground state calculated using accurate Hohenberg-Kohn-Sham density-functional (DF) techniques.[16,17] This is achieved by treating the atomic coordinates $\{\mathbf{R}_I\}$ and the electronic wave functions $\{\psi_i\}$, corresponding to occupied states, as dynamical degrees of freedom of a fictitious classical system described by the following equations of motion:[5]

$$\mu\ddot{\psi}_i(\mathbf{r},t) = -\frac{\delta E}{\delta\psi_i^*(\mathbf{r},t)} + \sum_j \Lambda_{ij}\psi_j(\mathbf{r},t) \equiv -H\psi_i(\mathbf{r},t) + \sum_j \Lambda_{ij}\psi_j(\mathbf{r},t) , \quad (1)$$

$$M_I\ddot{\mathbf{R}}_I = -\nabla_{\mathbf{R}_I} E . \quad (2)$$

Here dots indicate time derivatives, M_I denotes atomic masses, μ is an adjustable parameter setting the time scale for the fictitious electronic dynamics, Λ_{ij} are Lagrange multipliers used to satisfy the orthonormality constraints on the $\psi_i(\mathbf{r},t)$, and $E[\{\psi_i\},\{\mathbf{R}_I\}]$ is the DF energy functional with the local-density approximation for exchange and correlation,[16,17] supplemented with the direct ionic Coulomb repulsion.

$E[\{\psi_i\},\{\mathbf{R}_I\}]$ acts as the potential energy of the fictitious system. The BO surface Φ corresponds to the minimum of $E[\{\psi_i\},\{\mathbf{R}_I\}]$ with respect to the "electronic degrees of freedom" $\{\psi_i\}$:

$$\Phi[\{\mathbf{R}_I\}] = \min_{\{\psi_i\}} E[\{\psi_i\},\{\mathbf{R}_I\}] . \quad (3)$$

To solve Eqs. (1) and (2), the ground state Kohn-Sham orbitals for $\{\mathbf{R}_I(t=0)\}$, with velocities $\{\dot{\psi}_i(t=0)\}$ equal to zero, are taken as initial conditions for the electronic degrees of freedom, i.e., E is initially equal to Φ. Some energy transfer from the ionic to the electronic subsystem will then take place.[12] However, as far as the classical kinetic energy for the electronic degrees of freedom, $K_e = \sum_i \frac{1}{2}\mu \int d\mathbf{r}\,|\dot{\psi}_i|^2$ is much smaller than the ionic kinetic energy $K_I = \sum_I \frac{1}{2}M_I|\dot{\mathbf{R}}_I|^2$, electrons are very close to the ground state, i.e., E is very close to the BO surface Φ, and Eq. (2) describes physical atomic trajectories. Experience has shown that in insulators, by appropriate choice of μ, it is possible to make the time scale of the energy transfer so long that no systematic deviation from the BO surface occurs during typical MD simulation times. In metals, vice versa, some energy transfer on a relatively small time scale is found to occur for any choice of μ. In order to maintain the ions close to the BO surface, one has therefore to perform periodic electronic minimizations. Correspondingly, because of the energy loss in the ionic subsystem, one should couple the ions

to some external reservoir in order to maintain the temperature at the required value. In this work the ionic temperature is kept constant by using the scheme proposed by Nosé.[18]

Following Nosé,[18,19] we couple all ions of a given type α (α = Ga, As) to an extra degree of freedom s_α, the so-called "Nosé's thermostat" (the use of a different thermostat for each atomic species was found convenient to reduce the equilibration time). We thus replace Eq. (2) by the set of equations

$$M_{I,\alpha}\ddot{\mathbf{R}}_{I,\alpha} = -\nabla_{\mathbf{R}_{I,\alpha}} E - M_{I,\alpha}(\dot{s}_\alpha/s_\alpha)\dot{R}_{I,\alpha} \ , \tag{4}$$

$$Q_\alpha \ddot{s}_\alpha = s_\alpha \sum_I M_{I,\alpha}\dot{R}^2_{I,\alpha} - s_\alpha g_\alpha k_B T_{\rm eq} + Q_\alpha \dot{s}^2_\alpha/s_\alpha, \tag{5}$$

where Q_α can be thought of as the fictitious mass associated with s_α, g_α is the number of degrees of freedom in the physical system ($g_\alpha = 3N_\alpha$, N_α being the number of ions of species α), k_B is Boltzmann's constant, and $T_{\rm eq}$ is the externally set temperature value. Note that Eqs. (4) and (5) are written in terms of "real variables,"[18] so that the dots here indicate derivatives with respect to the "real time."

The coupled set of Eqs. (1), (4), and (5) lead to conservation of the energy of the extended system composed by the electrons, the ions, and the thermostats, $U_{\rm ext} = K_e + K_I + E + \frac{1}{2}\sum_\alpha Q_\alpha(\dot{s}_\alpha/s_\alpha)^2 + \sum_\alpha g_\alpha k_B T_{\rm eq} \ln s_\alpha$. However, as pointed out by Nosé,[18,19] $U_{\rm ext}$ is not a Hamiltonian and Eqs. (1), (4), and (5) cannot be derived from it directly. One can obtain instead these equations following the procedure decribed by Nosé for the case of multiple temperature control variables.[19] In particular one should assume that the ions are coupled to the variables s_α, while the electrons have no thermal bath.

If the potential energy E in Eq. (4) is given by the BO potential-energy surface Φ, then, as shown by Nosé,[18] Eqs. (4) and (5) lead to a canonical distribution in the ionic phase space. To achieve this situation, one can in principle perform an electronic minimization at each ionic time step. This, however, would be very costly and in practice it is not necessary because, using the dynamical equation (1), the electrons remain very close to the ground state for many time steps. Thus the conditions for the approximate sampling of the canonical distribution remain valid also in this case. We found that using a Verlet algorithm[20] with a time step Δt=15 a.u. ($\sim 3.6\times10^{-16}$ sec), and the fictitious mass parameter of the electronic degrees of freedom μ=7500 a.u., it was sufficient to perform the minimizations every 200 Δt. Within this time scale, K_e slowly increases up to $\sim$ 0.03 a.u., corresponding to an "electronic temperature" $T_e \equiv 2K_e/3Nk_B$ (N being the total number of atoms) of $\sim$ 100 K, and thus much smaller than the equilibrium temperature of the real system, $\sim$ 1600 K (see Sec. II). The periodic minimizations of the electronic degrees of freedom were performed using an efficient conjugate gradients procedure.[21]

Although, in principle, the value of Q_α is arbitrary, too small Q_α values may give decoupling of s_α from the physical system, whereas too large Q_α values lead to insufficient sampling of phase space. Based on physical considerations, Nosé has suggested choosing[18]

$$Q_\alpha = \frac{2g_\alpha k_B T_{\rm eq}}{\omega^2 < s_\alpha >^2} \ , \tag{6}$$

where ω is of the order of the second moment of the frequency spectrum of the velocity autocorrelation function of the physical system. With this choice, the dynamics of the variable s_α is on the same time scale as that of the physical system. The values of Q_α used in this work are $Q_\alpha = 1.15 \times 10^6$ a.u. (the same value is used for both thermostats).

III. DETAILS OF THE CALCULATION

A. Pseudopotentials for Ga and As and the Kleinman-Bylander scheme

In this work, the norm-conserving pseudopotentials (NCPS) (Ref. 13) obtained by Bachelet *et al.*[14] are employed for Ga and As, where $1s2s2p3s3p3d$ states are treated as core states. These pseudopotentials have the form

$$\hat{V}_{\rm ps} = \sum_l v_l(r)\hat{P}_l, \tag{7}$$

where $\hat{P}_l$ is a projection operator onto the lth angular-momentum component. We assume

$$v_l(r) = v_{\rm ref}(r) \ \ \text{for } l > l_{\rm max}, \tag{8}$$

where $v_{\rm ref}$ is a reference potential, usually the $l = 2$ term of Eq. (7) for sp-bonded systems. Equation (7) then becomes

$$\hat{V}_{\rm ps} = v_{\rm ref}(r) + \sum_{l=0}^{l_{\rm max}} \Delta v_l \hat{P}_l, \tag{9}$$

where $\Delta v_l = v_l - v_{\rm ref}$ is zero outside the core. Since the high-l components of the wave functions have little weight inside the core, the choice of $v_{\rm ref}$ is largely arbitrary. In Eq. (9), the first term on the right-hand side is a local operator $\hat{V}_{\rm loc}$, while the rest is the nonlocal (NL) part, $\hat{V}_{\rm NL}$.

A few years ago, Kleinman and Bylander (KB) (Ref. 15) proposed a factorized form for the NL pseudopotentials which reduces significantly the effort of calculating the NL pseudopotential elements. In the KB scheme the pseudopotential is written as

$$\hat{V}_{\rm NL} = \sum_l^{l_{\rm max}} \sum_m \frac{|\Delta v_l \Phi^0_{lm} >< \Phi^0_{lm} \Delta v_l|}{< \Phi^0_{lm}|\Delta v_l|\Phi^0_{lm} >} \ , \tag{10}$$

where Φ^0_{lm} are atomic pseudo-wave-functions corresponding to the pseudopotential of Eq. (7).

The KB scheme is computationally very convenient, especially when used within iterative schemes, as the one defined in Eq. (1).[21,22] However, as dicussed in detail by various authors,[23,24] it is found that the accuracy of the scheme depends strongly on the choice of the reference function in Eq. (9). In the following we shall present the results of several tests aimed at finding an appropriate reference potential for the KB scheme in GaAs.

1. Testing the KB scheme for c-GaAs

Our tests were performed on crystalline GaAs (*c*-GaAs). For a given choice of the reference potential of Ga and As, we calculated the energy eigenvalues within the Kohn-Sham local-density approximation (LDA) (Ref. 17) by using both the standard unfactorized formula[25] (we denote these results as "exact") and the factorized KB expression (10). The **k** points in the first BZ used to represent the charge density within the Hohenberg-Kohn DF scheme are those which fold into the Γ point of the cubic supercell of 64 atoms used in our subsequent calculations for the liquid (see Sec. III B). Very similar eigenvalues are obtained with a converged set of special **k** points.[26] We used for the wave functions a plane-wave (PW) representation with an energy cutoff of 14 Ry (~140 PW's per atom), which yields reasonably well-converged energy eigenvalues.[26] Given this choice for the wave functions, we found that a cutoff of 14×1.58 Ry=22.12 Ry was sufficient to represent very accurately the charge density and the potential.

We tested two different reference potentials, i.e., $v_{\mathrm{ref},\alpha} = v_{2,\alpha}$ (d potential) and $v_{\mathrm{ref},\alpha} = v_{1,\alpha}$ (p potential), where α = Ga, As. In the first case $\hat{V}_{\mathrm{NL}} = \Delta v_0 \hat{P}_0 + \Delta v_1 \hat{P}_1$ (we denote it as *sp*-NL) whereas in the second case $\hat{V}_{\mathrm{NL}} = \Delta v_0 \hat{P}_0 + \Delta v_2 \hat{P}_2$ (we denote it as *sd*-NL). Our results are given in Table I.

From Table I, we can see that, unlike the "exact" results, the KB scheme is quite sensitive to the choice of the reference potential.[15,27] In particular, it appears that while the KB scheme with *sd*-NL agrees quite closely with the exact results, in the *sp*-NL case the KB eigenvalues deviate appreciably from the exact ones. In the latter case, the most important difference occurs for the first conduction band, and in particular for the energy gap between the valence and conduction bands ($\Gamma_1 - \Gamma_{15}$), which is only ~ 0.25 the value of the exact one. (Of course, the exact itself is smaller than the experiment, as usually found in DF calculations.) This large underestimate of the gap may have consequences whenever deviations from perfect crystalline order occur, and therefore the choice of *sp*-NL within the KB scheme should be avoided for GaAs.

A further choice for the reference potentials is suggested by Fig. 1. Here we show the NL terms of the pseudopotential, v_l, for Ga and As.[14] It is evident that the $v_2(r)$ and $v_1(r)$ potentials for Ga are quite close. Thus, we take approximately $v_2 \simeq v_1$ for Ga, i.e., we treat Ga as *s*-NL but As as *sp*-NL. The energy eigenvalues obtained with this choice of the reference potentials are listed in Table II. It appears that the KB results are quite close to the exact ones. (The difference between the exact results of Tables I and II should be related to the different potential for the Ga d electrons: this is more attractive in the case of Table II.) This choice, which has the advantage of being rather accurate and computationally convenient, is the one which we shall adopt in the following.

The effect of the different forms of NL pseudopotentials can be illustrated by the calculated lattice constants of *c*-GaAs. The lattice constant, computed employing *s*-

TABLE I. Energies (in units of eV) at some selected **k** points for *c*-GaAs, obtained by the "exact" and the KB scheme. The sixth column reports experimental results (Ref. 26).

	sp-NL		*sd*-NL		
k	exact	KB	exact	KB	Expt.
Γ_1	−12.56	−12.69	−12.55	−12.55	−13.1
Γ_{15}	0	0	0	0	0
Γ_1	0.62	0.15	0.63	0.72	1.42
Γ_{15}	3.75	3.77	3.75	3.76	
X_1	−10.14	−10.13	−10.13	−10.13	−10.75
X_3	−6.72	−6.79	−6.72	−6.72	−6.70
X_5	−2.59	−2.57	−2.59	−2.58	−2.80
X_1	1.41	1.03	1.41	1.43	1.81
X_3	1.61	1.46	1.61	1.62	2.38
X_5	10.15	10.16	10.16	10.17	
L_1	−10.90	−10.94	−10.89	−10.89	−11.24
L_1	−6.54	−6.57	−6.54	−6.53	−6.70
L_3	−1.09	−1.08	−1.09	−1.09	−1.30
L_1	1.03	0.54	1.04	1.08	1.72
L_3	4.62	4.62	4.62	4.62	5.41
L_1	7.68	5.26	7.70	7.71	

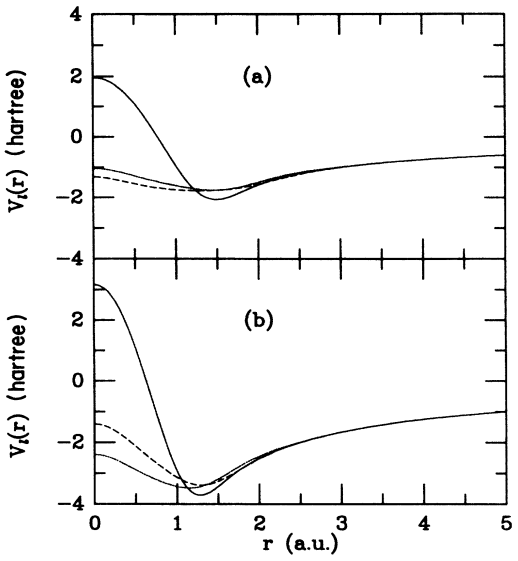

FIG. 1. NL terms of the pseudopotential for (a) Ga and (b) As (Ref. 14). The solid, dashed, and dotted curves correspond to s, p, and d potentials, respectively.

NL for Ga and sp-NL for As, is ~10.35 a.u., i.e., 3% smaller than the experimental value [10.68 a.u. (Ref. 28)], whereas if both Ga and As are treated as sp-NL the lattice constant is ~10.45 a.u., i.e., 2% smaller than the experiment (the same results are found both with the exact and the KB schemes). We see no essential difference.

TABLE II. Energies (in units of eV) of c-GaAs at some selected **k** points using sp-NL for As and only s-NL for Ga. The three columns refer to three different treatments of the NL pseudopotential. The symbol in parentheses denotes which wave function is used in the KB formula.

k	exact	KB(Φ^0_{lm})	KB($\tilde{\Phi}_{lm}$)
Γ_1	−12.32	−12.30	−12.28
Γ_{15}	0	0	0
Γ_1	0.86	1.09	1.01
Γ_{15}	3.94	3.95	3.95
X_1	−9.96	−9.96	−9.95
X_3	−6.52	−6.53	−6.53
X_5	−2.38	−2.38	−2.39
X_1	1.44	1.49	1.47
X_3	1.64	1.65	1.65
X_5	10.30	10.20	10.21
L_1	−10.70	−10.70	−10.68
L_1	−6.32	−6.32	−6.33
L_3	−0.97	−0.96	−0.97
L_1	1.19	1.28	1.25
L_3	4.64	4.64	4.64
L_1	7.85	7.83	7.84

2. Using the KB scheme for ab initio molecular dynamics

A drawback of using the KB potential within the *ab initio* MD scheme is that an instability is sometimes found in the numerical solution of the equations of motion (1).[29] More precisely, it turns out that the time step Δt must be restricted to very small values for a correct numerical integration of the equations of motion. This makes the calculations more costly and somehow offsets the advantages of the KB scheme.

Such an instability appears to be related to the denominator of Eq. (10). Other instabilities of the KB scheme which may be caused by the small value of this denominator, e.g., the occurrence of "ghost" states, have been discussed in the literature.[23,24] The instability that we have found, although of similar origin, is more directly related to the use of the KB potential within the iterative scheme of this work, and has not been discussed previously. In our case, as described in Sec. II, $H\psi$ works as the force on the electronic degrees of freedom. If one or more denominators in the KB formula happen to be very small, some forces will become very large in magnitude, so that a very small Δt is needed. This case happens indeed for As when we use v_2 or v_1 as the reference potential.

The justification of the KB scheme is based on the fact that when the KB-NL pseudopotential acts on a state Ψ equal to the atomic state Φ^0_{lm}, it is equivalent to the exact one

$$\frac{|\Delta v_l \Phi^0_{lm}><\Phi^0_{lm}\Delta v_l|}{<\Phi^0_{lm}|\Delta v_l|\Phi^0_{lm}>}|\Psi\equiv\Phi^0_{lm}>=|\Delta v_l\Phi^0_{lm}> \ . \tag{11}$$

In our calculations, the state Ψ is given in terms of a truncated PW expansion, i.e.,

$$\Psi(\mathbf{r})=\sum_{G=0}^{G_{max}} c_G e^{i\mathbf{G}\cdot\mathbf{r}} \ . \tag{12}$$

It appears that in order to satisfy the equality (11), the function Φ^0_{lm} appearing in the KB factorized potential must be changed consistently to $\tilde{\Phi}^0_{lm}$, which is obtained by truncating the PW expansion of Φ^0_{lm}, i.e.,

$$\tilde{\Phi}^0_{lm}(\mathbf{r})=\sum_{G=0}^{G_{max}} c^0_G e^{i\mathbf{G}\cdot\mathbf{r}} \ . \tag{13}$$

We found that when this is done, the "instability problem" mentioned above is also largely removed. In our calculations, for instance, the value of the time step Δt for the integration of Eq. (1) could be increased by a factor 3 by this change (leaving the electronic fictitious mass μ unchanged). In the third column of Table II, we report selected eigenvalues of c-GaAs calculated using the KB-$\tilde{\Phi}$ scheme. It appears that the comparison with both the KB using true atomic states and the exact scheme is very favorable.

B. MD cell and preparation of the liquid

A cubic MD cell containing 64 (32 Ga and 32 As) atoms with periodic boundary conditions is used. The cell size is chosen as 20.864 a.u., giving the experimental density at the melting point, $\rho \sim 5.71$ gr cm^{-3}.[3] The electronic wave functions at the Γ point in the first BZ are expanded in PW's with a kinetic-energy cutoff of 14 Ry, corresponding to more than 8000 PW's per state. The NCPS discussed in the previous section[13,14] are used together with the factorized form of Kleinman and Bylander of the nonlocal pseudopotentials.[15] Due to the reason explained above (Sec. II A), s nonlocality for Ga and sp nonlocality for As are adopted.

To prepare the liquid, the atoms are initially arranged in a zinc-blende crystal structure with some random displacements. The temperature of the system is gradually raised (by rescaling the ionic velocities) up to 3000 K, until the mean square displacement shows the diffusive behavior typical of a liquid. The temperature is then gradually reduced to ~1600 K, somewhat above the experimental melting point 1511 K. The system is equilibrated at this temperature for a few thousand time steps, after which statistics is collected for 4800 time steps (~1.72 ps). The rms temperature fluctuation during the run is $\Delta T \sim 200$ K.

IV. RESULTS AND DISCUSSION

A. Structural properties

From the ionic coordinates of the configurations collected in the simulation, we obtain the so-called Asfcroft and Langreth (AL) partial pair correlation functions $g_{\alpha\beta}(r)$ and structure factors $S_{\alpha\beta}(k)$ (α = Ga, As; β = Ga, As), defined as[30]

$$c_\beta \rho g_{\alpha\beta}(r) = \frac{1}{N_\alpha} < \sum_{I=1}^{N_\alpha} \sum_{J=1}^{N_\beta} \delta(\mathbf{r} - (\mathbf{R}_{\alpha I} - \mathbf{R}_{\beta J})) > -\delta_{\alpha\beta}\delta(\mathbf{r}) , \tag{14}$$

$$S_{\alpha\beta}(k) = (N_\alpha N_\beta)^{-1/2} < \sum_{I=1}^{N_\alpha} \sum_{J=1}^{N_\beta} \exp(-i\mathbf{k}\cdot(\mathbf{R}_{\alpha I} - \mathbf{R}_{\beta J})) > -(N_\alpha N_\beta)^{1/2}\delta_{\mathbf{k},0} , \tag{15}$$

where N_α is the number of α-type atoms and $c_\alpha = N_\alpha/N$ is the corresponding number concentration.

To compare our results with the neutron-scattering experiment,[1] we combine the partial $S_{\alpha\beta}(k)$ with the experimental neutron-scattering lengths b_α as follows:

$$S(k) = \frac{b_{\mathrm{Ga}}^2 S_{\mathrm{GaGa}}(k) + 2b_{\mathrm{Ga}}b_{\mathrm{As}}S_{\mathrm{GaAs}}(k) + b_{\mathrm{As}}^2 S_{\mathrm{AsAs}}(k)}{b_{\mathrm{Ga}}^2 + b_{\mathrm{As}}^2} , \tag{16}$$

where $b_{\mathrm{Ga}} = 7.2$ and $b_{\mathrm{As}} = 6.7$.[2] The comparison for the structure factor $S(k)$ is shown in Fig. 2. It appears that, although the calculated $S(k)$ is somewhat noisy because of the limited statistics, the agreement between theory and experiment is quite good. In particular, the theoretical curve reproduces well the width of the first peak of $S(k)$, which, as in l-Si and l-Ge, is very broad in comparison with that of most liquid metals. However, finer details of the experimental curve, such as the shoulder of the first peak at high k's, are not described as well. The small shift of the calculated $S(k)$ to higher k-value with respect to the experiment is due to the theoretical underestimate of the Ga—As equilibrium bond length which was mentioned in Sec. II.

In Fig. 3 we show the partial structure factors of Bhatia and Thornton,[31] defined as

$$S_{NN}(k) = \frac{1}{N} < N^*(\mathbf{k})N(\mathbf{k}) > , \tag{17a}$$

$$S_{CC}(k) = N < C^*(\mathbf{k})C(\mathbf{k}) > , \tag{17b}$$

$$S_{NC}(k) = \mathrm{Re} < N^*(\mathbf{k})C(\mathbf{k}) > , \tag{17c}$$

where $N(\mathbf{k})$ and $C(\mathbf{k})$ are the Fourier transforms of the local fluctuations of the number density

$$\Delta\rho(\mathbf{r}) = \rho(\mathbf{r}) - \bar{\rho} \tag{18}$$

and the concentration

$$\Delta c(\mathbf{r}) = c(\mathbf{r}) - \bar{c} , \tag{19}$$

respectively. From Fig. 3, it appears that $S_{NN}(k)$ is very similar to $S(k)$ of Fig. 2, and $S_{CC}(k)$ has a broad peak at ~ 1.8 Å^{-1}, i.e., at about half of the position of the first peak of $S_{NN}(k)$, revealing a tendency to an alternative arrangement of atoms, although this is not as pronounced

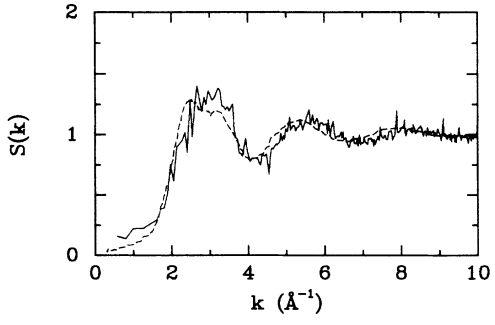

FIG. 2. Structure factor of l-GaAs. Solid line, calculated curve; dashed line, neutron-scattering results (Ref. 1).

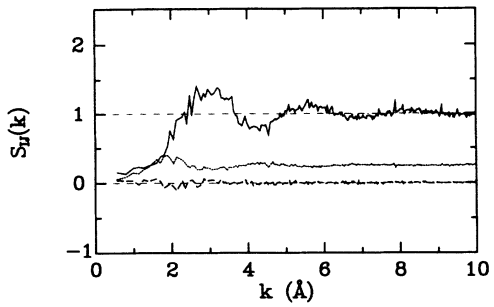

FIG. 3. Number-concentration structure factors S_{IJ} $(I, J = N, C)$. Solid line, S_{NN}; dotted line, S_{CC}; dashed line, S_{NC}.

as that in a pure ionic system.

Better insight into the structure of the liquid is provided by the pair correlation function $g(r)$. In Fig. 4(a), the experimental $g(r)$, which was obtained by Fourier transformation of the experimental $S(k)$, and our result are shown. This is obtained by weighting the partial $g_{\alpha\beta}(r)$—which are calculated directly in r space—with the b_α's, in a way similar to that of Eq. (16). A noticeable feature of both curves in Fig. 4(a) is the almost complete absence of structure beyond the first neighbor peak. This feature is usually attributed to noncompact structures, since in these systems the structure is not "nested" shell by shell. It also appears that, in spite of an inward shift which corresponds to the outward shift in $S(k)$, the theoretical peak reproduces quite well the height and width of the experiment. From the area below the first peak of $g(r)$, one can estimate the average coordination number z in the liquid. By fitting the first peak with two Gaussians, we find $z = 5.0$, whereas by direct integration of $4\pi\rho r^2 g(r)$ up to the first minimum at $r_{\min} \sim 3.26$ Å, we find $z = 6.3$. The corresponding experimental value is $z = 5.5 \pm 0.5$, the incertitude being related to the procedure used to analyze the first peak. An overall good agreement with the experimental $g(r)$ was recently obtained also by Hafner and Jank.[10] Their calculated $g(r)$, however, is more structured beyond the first peak, indicating an overestimate of medium-range correlations.

The calculated partial pair correlation function $g_{\alpha\beta}(r)$ is shown in Fig. 4(b). As discussed in the Introduction, experimental results for these quantities are not available, although in principle they can be obtained by scattering through isotopic substitution. In strongly ionic systems, such as molten salts, peaks and minima of $g_{\alpha\beta}(r)$ for like atoms are out of phase with respect to those of unlike atoms, reflecting the characteristic alternation of cation and anion shells. This is not the case in Fig. 4(b), indicating a prominent covalent character for the binding in l-GaAs. By integrating $g_{\alpha\beta}(r)$ to $r_{\min}$, we find that each Ga/As has on the average 2.6/2.2 and 3.9 neighbors of the like and unlike species, respectively. Although the probability of finding a like atom in the nearest-neighbor shell of one atom is appreciable, the As-Ga correlations are clearly dominant. This is at variance with the chemically random atomic distribution obtained in Ref. 10.

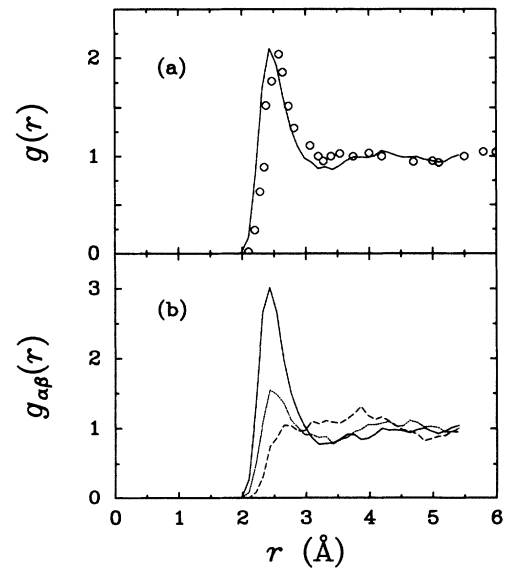

FIG. 4. (a) Pair correlation function $g(r)$. Solid line, calculated curve; circles, experimental results. (b) Partial correlation functions. Solid line, Ga—As; dashed line, As—As; dotted line, Ga—Ga.

B. Dynamical properties

The dynamical properties of the liquid[32] are well described by our simulation. The diffusion coefficients of Ga and As can be evaluated from the large t behavior of mean square displacements by the Einstein relation

$$D = \lim_{t\to\infty} < r^2 > /6t \tag{20}$$

as $D_{\mathrm{Ga}} = 1.6 \times 10^{-4}$ cm^2 s^{-1} and $D_{\mathrm{As}} = 1.2 \times 10^{-4}$ cm^2 s^{-1}, respectively. The same value is obtained from the integral of the autocorrelation function of the atomic velocity

$$Z(s) = \frac{< \mathbf{V}(t) \cdot \mathbf{V}(t+s) >}{< \mathbf{V}(t) \cdot \mathbf{V}(t) >} . \tag{21}$$

The experimental value, which does not distinguish between the two different species, is $D_{\mathrm{GaAs}} = 1.6 \times 10^{-4}$ cm^2 s^{-1} at $T \sim 1550$ K.[33]

The vibrational density-of-states spectrum $D(\nu)$ is obtained by Fourier transformation of $Z(s)$, i.e.,

$$D(\nu) \propto \int_0^\infty Z(t) \cos(2\pi\nu t) dt, \tag{22}$$

and is shown in Fig. 5. A shoulder occurs at about $\nu \sim 4$ THz which should be related to the optical phonon peak

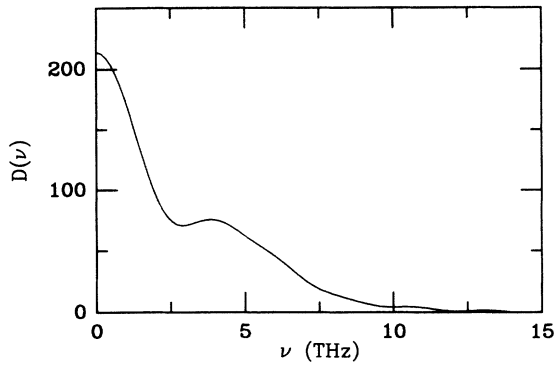

FIG. 5. Vibrational density of states. The unit for $D(\nu)$ is arbitrary.

in the crystal. This value is $\nu \sim 8$ THz at zero temperature. As temperature rises, it will shift to lower value. Unfortunately no experimental data near the melting point seem available.

C. Covalent (weakly ionic) bonds and broken bonds

The value of z in l-GaAs is much lower than that of most liquid metals, and even lower than that in l-Si and l-Ge. Such a low coordination suggests that covalent bonds similar to those of c-GaAs may still be present in the liquid. To investigate this question, we have performed an extensive analysis of the charge distribution, which in the *ab initio* MD scheme is generated together with the atomic trajectories. In Fig. 6 we show contour plots of the charge density for a few typical configurations of the liquid, as compared to the charge density [in a (110) plane] of c-GaAs. It appears that covalent (weakly ionic) bonds are indeed formed provided the interatomic distance d is below some value $d_{\rm cov}$, which we approximately estimate as $d_{\rm cov} \sim 2.65$ Å, i.e., $\sim 10\%$ larger than the equilibrium bond length for c-GaAs (we assume the same $d_{\rm cov}$ for all types of bond, although the average As-As separation is found to be slightly larger than the Ga-As and Ga-Ga ones). By integrating $g(r)$ up to $d_{\rm cov}$ we obtain that the average number of bonds formed by each atom is ~ 2.9, implying that about 50% of the atoms within the first coordination shell of radius $r_{\rm min}$ are, on the average, bonded to the central atom. A similar type of analysis applied to l-Si shows that only $\sim 30\%$ of the atoms of the first coordination shell form bonds with the central atom.[7]

The occurrence of bonds in l-GaAs is confirmed by the behavior of the bond-angle distribution (AD). Figure 7 shows the total AD calculated using two different values of the cutoff distance R_c, namely $R_c = r_{\rm min}$ and $R_c = d_{\rm cov}$ (dashed line). A significant difference between the two curves is remarkable. It appears that the curve with $R_c = d_{\rm cov}$ has a pronounced peak at $\theta \sim 109°$, i.e., the bond angle of c-GaAs, whereas for the curve with $R_c = r_{\rm min}$ the peak has become broader and shifted to $\theta \sim 100°$, while at the same time a second feature at $\theta \sim 54°$ has emerged. The latter corresponds to configurations where at least one atom within $r_{\rm min}$ is not bonded to the central one.

Charge-density contour plots for several bonding configurations in the liquid are shown in Fig. 8, including "crystal-like" configurations such as (a) and (d), wrong bonds such as in (b) and (e), and three-atom "clusters" as in (c) and (f). The "crystal-like" configurations of type (a) and (d) are the prominent configurations, but configurations like (b) and (e) also occur frequently. We find statistically that about 18 and 9% of the total num-

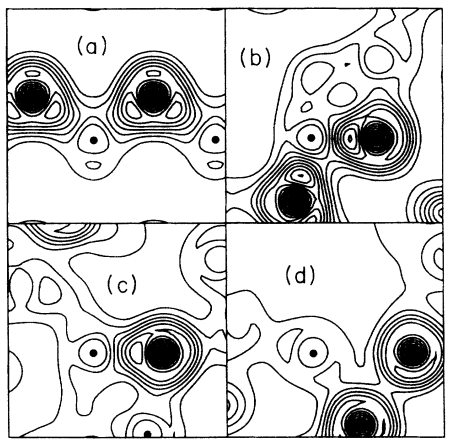

FIG. 6. Contour plots of the valence electronic-charge density. Small and large dots denote Ga and As ions, respectively. (a) Charge density in the (110) plane of c-GaAs (bond length $d_c = 2.45$ Å). (b), (c), and (d) are some selected configurations of the liquid. In (b), both As atoms form bonds with the Ga atom at the center (bond distances: $d_1 \simeq d_2 = 2.14$ Å). In (c) the As atom bonds to the Ga on the left ($d_1 = 2.21$ Å) while it does not form a bond with the Ga at the bottom ($d_2 = 2.70$ Å). In (d) the Ga atom does not form bonds with either As atom ($d_1 = 3.22$ Å, $d_2 = 2.81$ Å).

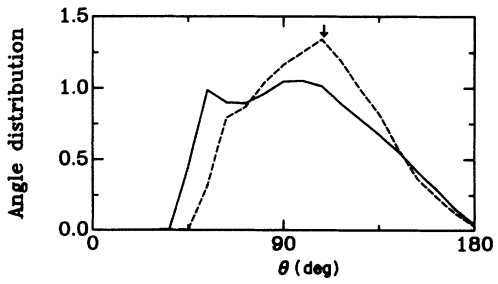

FIG. 7. Total bond-angle distribution calculated using two different values of the cutoff distance R_c, $R_c = r_{\rm min}$ (solid line) and $R_c = d_{\rm cov}$ (dashed line). The vertical arrow denotes the value of the tetrahedral angle, 109°.

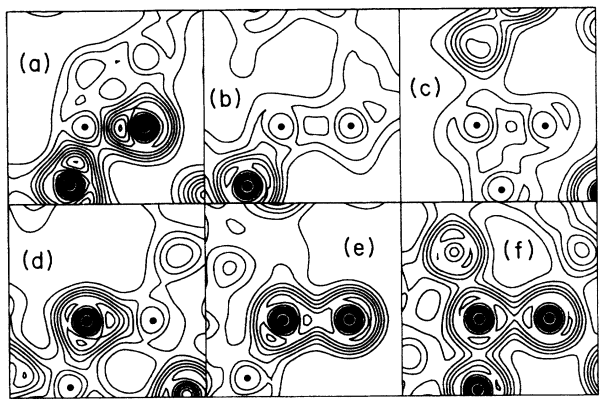

FIG. 8. Contour plots of the valence electronic-charge density in l-GaAs for different atomic configurations: (a) Ga-As-Ga; (b) Ga-Ga-As; (c) Ga-Ga-Ga; (d) Ga-As-Ga; (e) As-As-Ga; (f) As-As-As. The small and large dots denote Ga and As ions, respectively.

ber of bonds are Ga—Ga and As—As, respectively. The probability of the "three-atom cluster" configurations (c) and (f) is instead significantly lower (4 and 2%, respectively). "Clusters" with atoms larger than 4 only occur occasionally.

The charge-density plots in Fig. 8 also show that the Ga—As bond in the liquid is weakly ionic, as in the crystal. The Ga—Ga bond shows a small pileup of charge at the center, similar to that observed in orthorhombic c-Ga.[34] Finally, the As—As bond is dominated by p electrons as found in c-As.[35] Correspondingly, we find that the partial AD for AsGaAs is peaked at $\sim$ 105°, i.e., rather close to the tetrahedral angle of 109°, and that for AsAsAs has a sharp peak at $\sim$ 95°, i.e., rather close to the bond angle in pure l-As (Ref. 36) or c-As.[35] In contrast, the AD's for configurations such as GaAsGa and GaGaGa are found to be quite flat, suggesting weak interactions between the endpoint Ga atoms.

D. Electronic properties

We calculate the single-particle density of states and the electrical conductivity by averaging over 12 different ionic configurations $\{\mathbf{R}_I\}$. The lowest 256 Kohn-Sham states at Γ are used for each set of $\{\mathbf{R}_I\}$, i.e., twice the number of occupied states. These are found to give a good description of the spectrum up to $\sim 5-6$ eV above the Fermi energy. They are calculated using a conjugate-gradient minimization procedure similar to that used to determine the ground state.[21]

In Fig. 9 we show the density of states $D(E)$ of l-GaAs, together with the partial contributions $D_{s,\alpha}(E)$ and $D_{p,\alpha}(E)$ of s and p states centered on As and Ga atoms. The latter have been obtained by expanding our PW basis set into spherical waves centered on the various atoms, with a cutoff radius of $\sim$ 3 a.u. (results do not change for reasonable variations of this value). Some

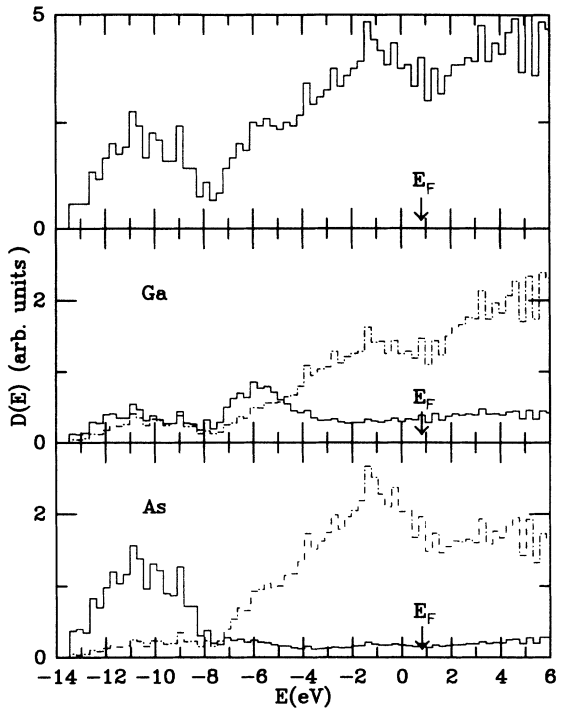

FIG. 9. Upper panel, electronic density of states $D(E)$; middle panel, $D_{s,\mathrm{Ga}}(E)$ (solid line) and $D_{p,\mathrm{Ga}}(E)$ (dash-dotted line) from s and p states centered on Ga atoms; lower panel, same as above for As. The vertical arrow denotes the position of the Fermi energy. The energy resolution of the histograms is 0.27 eV.

similarity of the density of states of the liquid to that of c-GaAs (Ref. 37) is visible. Also in the liquid, for instance, there is at low energies, between ~ -12 and ~ -8 eV, the band of s-like states originating from the As atoms, while the band between ~ -8 and ~ -4 eV is dominated by bonding states between Ga-s and As-

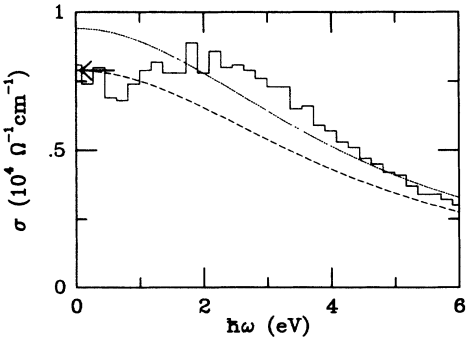

FIG. 10. Electrical conductivity $\sigma(\omega)$. Solid line, calculated curve; dashed and dotted lines, Eq. (24) with different values of σ_0 and τ (see text). The horizontal arrow indicates the experimental value of the dc conductivity. The energy resolution of the calculated curve is 0.18 eV.

p states. In the liquid, however, $D(E)$ is finite at the Fermi energy E_F within our energy resolution (ΔE = 0.01 a.u. = 0.27 eV is used for the histograms in Fig. 9), thus indicating that the liquid is metallic, in agreement with the experimental transport data.[3] (Obviously, for any fixed ionic configuration, there is a small, yet finite energy gap between filled and empty states, since our energy eigenvalue spectrum is discrete.)

The general features of the density of states in Fig. 9 were found to be substantially the same for all the different instantaneous ionic configurations that we have studied, which indicates that these are all equilibrium configurations and provide a representative sample of the liquid. This also suggests that the size of the system (64 atoms with periodic boundary condition) that we use to represent the liquid is sufficiently large. In such a situation, using the Γ point only to calculate $D(E)$ should be justified. This is also confirmed by the qualitative agreement between our results and the 4-**k**-points calculation by Hafner and Jank,[10] except for their additional band of very-low-lying Ga states, whose origin seems unclear. As compared to the density of states for l-Si,[7] our $D(E)$ for l-GaAs appears more structured.

In Fig. 10, we show the electrical conductivity $\sigma(\omega)$ calculated as the configurational average of the following Kubo-Greenwood formula:[38]

$$\sigma(\omega,\{\mathbf{R}_I\}) = \frac{2\pi e^2}{m^2\omega}\frac{1}{3\Omega}\sum_{m}^{\text{occ}}\sum_{n}^{\text{unocc}}\sum_{\alpha}|<\psi_m \mid \hat{p}_\alpha \mid \psi_n>|^2\delta(E_n - E_m - \hbar\omega)\ , \tag{23}$$

where occ and unocc denote filled and empty states, respectively (a sharp Fermi surface is assumed here, but we have checked that our results remain basically unchanged when Fermi occupation factors are introduced), and $\hat{p}_\alpha$ is the α ($\alpha = x, y, z$) component of the momentum operator. We remark that the use of Kohn-Sham states to evaluate Eq. (23) is not well justified,[39] and thus introduces an additional approximation, besides the neglect of nonadiabatic effects implicit in the use of BO states. In addition, in Eq. (23) the corrections to the momentum matrix elements introduced by the nonlocality of the ionic pseudopotentials are neglected.[40] The calculated value $\sim 7500\ \Omega^{-1}\,\text{cm}^{-1}$ of the static dc conductivity, obtained by extrapolating $\sigma(\omega)$ to zero frequency, is in remarkable agreement with the experimental value of $\sim 7900\ \Omega^{-1}\,\text{cm}^{-1}$.[3] However, due to the several approximations of our calculation, such a good agreement is to some extent fortuitous.

In the classical Drude model, the real part of the conductivity is

$$\sigma(\omega) = \frac{\sigma_0}{1+\omega^2\tau^2}\ , \tag{24}$$

where the relaxation time τ is related to the value σ_0 of the static conductivity by

$$\tau = \frac{m\sigma_0}{ne^2}\ , \tag{25}$$

m and n being the mass and density of the carriers, respectively. Using the experimental value of σ_0, the free-electron mass, and the density of valence electrons $n = 1.9 \times 10^{23}\ \text{cm}^{-3}$, we obtain $\tau = 1.5 \times 10^{-16}$ s. Although no experimental value of τ is available for l-GaAs, a value of the same order of magnitude, $\tau = 2.2 \times 10^{-16}$ s, has been measured in l-Si.[41] Equation (24), with $\sigma_0 = 7900\ \Omega^{-1}\,\text{cm}^{-1}$ and $\tau = 1.5 \times 10^{-16}$ s, is plotted as the dashed curve in Fig. 10. Significant differences between this curve and our calculations are evident. A somewhat better agreement between our results and the Drude expression can be obtained by treating σ_0 and τ in Eq. (24) as independent fitting parameters (see dotted curve in Fig. 10). From the fitting we obtain $\sigma_0 = 9400\ \Omega^{-1}\,\text{cm}^{-1}$ and $\tau = 1.5 \times 10^{-16}$ s. Using this value of τ, and the free-electron expression $l = \hbar k_F \tau/m$ for the mean free path, we find that the ratio l/a, where a is the average interparticle spacing, is $l/a \sim 1$, indicating a strong scattering behavior.[42] In l-Si the ratio l/a, estimated in a similar way, is somewhat larger, i.e., $l/a \sim 1.7$.[41]

V. SUMMARY AND CONCLUSIONS

In this paper we have presented the results of a first-principles MD simulation of liquid GaAs. In agreement with experiments, we have found that the liquid is metallic, with a coordination number between 5 and 6. From an extensive analysis of the electronic-charge density, we have shown that such a value of z, which is quite low as compared with that of most liquid metals, is related to the persistence of some covalent–weakly-ionic bonding effect in the liquid. On the average, almost 50% of the atoms of the first coordination shell are found to form bonds with the central atom. We have also investigated chemical ordering effects, and found that wrong bonds between like atoms have a rather high probability ($\sim 27\%$), but clustering is unlikely.

At variance with the crystal, these bonds have a finite lifetime caused by atomic diffusion. Whenever two atoms come sufficiently close to one another, a bond may be formed, which subsequently becomes weaker and finally disappears when the two atoms diffuse away. Similar bonding effects have been detected also in a recent *ab initio* molecular-dynamics simulation of l-Si.[7] For l-Si, however, the fraction of atoms in the first coordination shell which are bonded to the central atom is only 30%. This fact, together with the higher value of z, suggests a stronger metallic-like character of l-Si, as compared to l-GaAs.

The persistence of bonds similar to those of c-GaAs in the liquid is indicated by several other properties, such

as the bond-angle distribution, or the electronic single-particle density of states. The latter, for instance, is rather structured, and shows several features which are clear remnants of those in c-GaAs, such as the As-derived band of s-like states at the bottom of the valence band. Similarly, the optical conductivity of l-GaAs shows deviations from Drude-like behavior at low energies. The ratio l/a between the mean free path and the average interparticle spacing, estimated within a free-electron model, is ~ 1, which indicates a strong scattering situation. Better agreement with a Drude-like behavior is obtained for l-Si, and correspondingly l/a has a somewhat larger value, ~ 1.7. Some of these differences are likely to be related to the partial ionicity of the Ga—As bond, which is responsible, among others, for the wider average energy gap of c-GaAs with respect to that of c-Si.

ACKNOWLEDGMENTS

This work has been supported by the SISSA-CINECA (Scuola Internazionale Superiore di Studi Avanzati–Centro di Calcolo Elettronico dell'Italia Nord-Orientale) collaborative project, under the sponsorship of the Italian Ministry for Public Education, by Italian Consiglio Nazionale delle Ricerche (CNR) through Progetto Finalizzato Sistemi Informatici e Calcolo Parallelo, under Grant No. 89-00006-69, and by the European Research Office of the U.S. Army.

[1] C. Bergman, C. Bichara, P. Chieux, and J.P. Gaspard, J. Phys. Colloq. **C8-46**, 97 (1985).
[2] L. Koester, in *Neutron Physics*, Vol. 90 of *Springer Tracts in Modern Physics*, edited by G. Hohler (Springer-Verlag, Berlin, 1977).
[3] V.M. Glazov, S.N. Chizhevskaya, and N.N. Glagoleva, in *Liquid Semiconductors* (Plenum, New York, 1969).
[4] Y. Waseda, *The Structure of Non-Crystalline Materials; Liquids and Amorphous Solids* (McGraw-Hill, New York, 1980).
[5] R. Car and M. Parrinello, Phys. Rev. Lett. **55**, 2471 (1985).
[6] G. Galli, R.M. Martin, R. Car and M. Parrinello, unpublished.
[7] I. Štich, R. Car, and M. Parrinello, Phys. Rev. Lett. **63**, 2240 (1989).
[8] R. Car and M. Parrinello, Phys. Rev. Lett. **60**, 204 (1988).
[9] G. Galli, R.M. Martin, R. Car, and M. Parrinello, Phys. Rev. Lett. **62**, 555 (1989).
[10] J. Hafner and W. Jank, J. Phys. Condens. Matter **1**, 4235 (1989).
[11] R. Car, M. Parrinello, and W. Andreoni, in *Proceedings of the First NEC Symposium of Fundamental Approaches to New Material Phases*, edited by S. Sugano and S. Ohnishi (Springer-Verlag, Berlin, 1987).
[12] R. Car and M. Parrinello, in *Simple Molecular Systems at Very High Density*, edited by A. Polian, P. Loubeyre, and N. Boccara (Plenum, New York, 1989).
[13] D.R. Hamann, M. Schlüter, and C. Chiang, Phys. Rev. Lett. **43**, 1494 (1979).
[14] G.B. Bachelet, D.R. Hamman, and M. Schlüter, Phys. Rev. B **26**, 4199 (1982).
[15] L. Kleinman and D.M. Bylander, Phys. Rev. Lett. **48**, 1425 (1982).
[16] P. Hohenberg and W. Kohn, Phys. Rev. **136**, B864 (1964).
[17] W. Kohn, and L.J. Sham, Phys. Rev. **140**, A1133 (1965).
[18] S. Nosé, Mol. Phys. **52**, 255(1984); J. Chem. Phys. **81**, 511 (1984).
[19] S. Nosé, Mol. Phys. **57**, 187 (1986).
[20] L. Verlet, Phys. Rev. **159**, 98 (1967).
[21] I. Štich, R. Car, M. Parrinello, and S. Baroni, Phys. Rev. B **39**, 4997 (1989).
[22] D.C. Allan and M.P. Teter, Phys. Rev. Lett. **59**, 1136 (1987).
[23] D.M. Bylander and L. Kleinman, Phys. Rev. B **41**, 907 (1990).
[24] X. Gonze, P. Käckell, and M. Scheffler, Phys. Rev. B **41**, 12 264 (1990).
[25] J. Ihm, A. Zunger, and M.L. Cohen, J. Phys. C **12**, 4409 (1979).
[26] See, G.B. Bachelet and N.E. Christensen, Phys. Rev. B **31**, 879(1985), and references therein.
[27] D.R. Hamann, Phys. Rev. B **40**, 2980 (1989).
[28] R.C. Weast, in *Handbook of Chemistry and Physics*, 62nd ed. (CRC, Boca Raton,1988).
[29] D. Hohl, R.O. Jones, R. Car, and M. Parrinello, J. Chem. Phys. **89**, 6823 (1988).
[30] N.W. Ashcroft and D.C. Langreth, Phys. Rev. **156**, 685 (1967).
[31] A.B. Bhatia and D.E. Thornton, Phys. Rev. B **2**, 3004 (1970).
[32] For a general discussion of this subject, see, for instance, J.P. Hansen and I.R. McDonald, *Theory of Simple Liquids* (Academic, London, 1976).
[33] *Semiconductors: Physics of Group-IV Elements and III-V Compounds*, Vol. 17 of *Landölt-Bornstein: Numerical Data and Functional Relationships in Science and Technology*, edited by by K. -H. Hellwege (Springer-Verlag, Berlin, 1984), p. 341.
[34] X.-G. Gong, G. Chiarotti, M. Parrinello, and E. Tosatti, unpublished.
[35] L.F. Mattheiss, D.R. Hamann, and W. Weber, Phys. Rev. B **34**, 2190 (1986).
[36] R. Bellisent, C. Bergman, R. Ceolin, and J.P. Gaspard, Phys. Rev. Lett. **59**, 661 (1987).
[37] M.L. Cohen and J.R. Chelikowsky, *Electronic Structure and Optical Properties of Semiconductors* (Springer-Verlag, Berlin, 1988), p. 109.
[38] E.N. Economou, *Green's Functions in Quantum Physics*, Vol. 7 of *Springer Series in Solid State Sciences* (Springer, Berlin, 1983).
[39] See, for example, *Theory of Inhomogeneous Electron Gas*, edited by S. Lundqvist and N.H. March (Plenum, New York, 1983), and references therein.
[40] M.S. Hybertsen and S.G. Louie, Phys. Rev. B **35**, 5585 (1987).
[41] N.F. Mott and E.A. Davis, *Electronic Processes in Non-crystalline Materials* (Clarendon, Oxford, 1979).
[42] K.M. Shvarev, B.A. Baum, and P.V. Gel'd, Fiz. Tverd. Tela (Leningrad) **16**, 3246 (1974) [Sov. Phys.—Solid State **16**, 2111 (1975)].